Commun. Comput. Phys.
doi: 10.4208/cicp.171209.300710a

Vol. **9**, No. 4, pp. 897-916
April 2011

Exponential Compact Higher Order Scheme for Nonlinear Steady Convection-Diffusion Equations

Y. V. S. S. Sanyasiraju* and Nachiketa Mishra

Department of Mathematics, Indian Institute of Technology Madras, Chennai 600036, India.

Received 17 December 2009; Accepted (in revised version) 30 July 2010

Available online 13 October 2010

Abstract. This paper presents an exponential compact higher order scheme for Convection-Diffusion Equations (CDE) with variable and nonlinear convection coefficients. The scheme is $\mathcal{O}(h^4)$ for one-dimensional problems and produces a tri-diagonal system of equations which can be solved efficiently using Thomas algorithm. For two-dimensional problems, the scheme produces an $\mathcal{O}(h^4+k^4)$ accuracy over a compact nine point stencil which can be solved using any line iterative approach with alternate direction implicit procedure. The convergence of the iterative procedure is guaranteed as the coefficient matrix of the developed scheme satisfies the conditions required to be positive. Wave number analysis has been carried out to establish that the scheme is comparable in accuracy with spectral methods. The higher order accuracy and better rate of convergence of the developed scheme have been demonstrated by solving numerous model problems for one and two-dimensional CDE, where the solutions have the sharp gradient at the solution boundary.

AMS subject classifications: 65N05, 76M20, 35Q35

Key words: Finite difference, higher order, exponential compact, convection-diffusion.

1 Introduction

Convection-diffusion equation appears in the modelling of different fluid flow problems like contaminant transport and heat/mass transport etc. The traditional Finite Difference (FD) schemes such as central difference and upwind schemes on uniform grids have certain drawbacks viz. stability and/or accuracy, especially for convection dominated problems. Very large number of grid points are required to overcome such drawbacks and to obtain any reliable solution. In the last few years, Higher Order Compact (HOC) FD schemes have received great attention for solving CDE, which are computationally

*Corresponding author. *Email addresses:* sryedida@iitm.ac.in (Y. V. S. S. Sanyasiraju), mishra.nachiketa@gmail.com (N. Mishra)

efficient. All most all HOC schemes are either polynomial [1, 6, 8, 12, 14] or exponential type. For convection dominated problems polynomial schemes are less efficient due to the failure of discrete maximum principle and/or upwind effect in the scheme.

The finite difference methods, whose coefficients involve exponential functions of the coefficients of the corresponding differential operator and mesh width are known as exponentially fitted FD schemes [11]. HOC exponential schemes are the higher order compact exponentially fitted schemes. In the exponentially fitted FD schemes, the exponential function helps in introducing an artificial diffusion that preserves the upwind effect. Its coefficient matrix is unconditionally diagonally dominant. Such schemes are very suitable to solve the singularly perturbed convection-diffusion equations. Exponential FD schemes are first introduced by Allen and Southwell [2] to solve second order partial differential equations governing the transport of vorticity. Later, modified and improved schemes along with some analysis on their applicability are proposed in [4, 5, 10, 13, 15]. The more efficient as well as accurate scheme among the existing exponential HOC schemes is the SRECHOS [13]. So far SRECHOS has been developed for convection-diffusion equations with constant convection coefficients. Since most of the partial differential equations of practical importance have variable or nonlinear convection coefficients, therefore, the purpose of the present article is to develop and validate SRECHOS like scheme to CDE with variable and nonlinear convection coefficients. The development of the scheme is more or less in the lines of [15], however the final scheme differs from [15] as the present scheme does not require second-order derivatives of the source function in its implementation which will help in a substantial reduction in the CPU times and a better accuracy in some cases.

If SRECHOS [13] is applied directly to the CDE with variable convection coefficients, it will be of second order accurate. Using the method of modified equations, fourth order accurate scheme for CDE has been proposed in Section 2. The iterative scheme for the nonlinear CDE has been presented in Section 3. The positivity of the scheme, which is crucial for the convergence of the iterative scheme in solving the nonlinear CDE, has been shown in Section 4. The spectral analysis is also been presented in this section. Finally, all the schemes are experimentally verified with the existing schemes in Section 5 for variable, nonlinear and coupled nonlinear CDE.

2 Development of the scheme

Consider the two-dimensional nonlinear steady convection-diffusion equation

$$-au_{xx}-bu_{yy}+c(x,y,u)u_x+d(x,y,u)u_y=f(x,y), \tag{2.1}$$

on $\Omega\subset\mathbb{R}^2$, with boundary condition

$$u(x,y)=g(x,y), \quad \text{on } \partial\Omega, \tag{2.2}$$

where $a,b>0$ are constant diffusion, c,d are convection coefficients and f, g are sufficiently smooth functions with respect to x and y. If $0<a,b<1$ are very small when compared

with c and d, Eq. (2.1) is a convection dominated problem (i.e., singularly perturbed), and the solution may have a sharp boundary layer towards the inflow or outflow boundaries. Therefore the classical numerical methods may not be very accurate in resolving the high gradient solutions in the boundary layer regions.

2.1 One-dimensional case

To develop a higher order exponential scheme, first consider the one-dimensional linear equivalent of (2.1), given by

$$Lu \equiv -au_{xx}+c(x)u_x = f(x), \quad x \in I=(r_0,r_1), \tag{2.3a}$$

$$u(r_0)=\Gamma_0, \qquad u(r_1)=\Gamma_1. \tag{2.3b}$$

Divide the interval $[r_0,r_1]$ into n equal sub-intervals with $x_i=r_0+ih$, $h=x_{i+1}-x_i$, $u_i=u(x_i)$, $c_i=c(x_i)$, $f_i=f(x_i)$ and $i\in\{0,1,2,\cdots,n\}$.

The differential equation in (2.3), at any grid point x_i is replaced with a difference equation given by

$$-\alpha D_h^2 u_i + cD_h u_i = p_1 f_{i-1}+p_2 f_i + p_3 f_{i+1}+p_4 f_{x_{i-1}}+p_5 f_{x_i}+p_6 f_{x_{i+1}}, \tag{2.4}$$

where f_x is the derivative of f with respect to x, $D_h u_i=(u_{i+1}-u_{i-1})/2h$ and $D_h^2 u_i = (u_{i+1}-2u_i+u_{i-1})/h^2$. Replacing f with $(-au_{xx}+cu_x)$ and making Eq. (2.4) exact for x, x^2, x^3, x^4, x^5, x^6 and $e^{(cx/a)}$, gives $\alpha=a$, $p_1=2/15$, $p_2=11/15$, $p_3=2/15$, $p_4=h/40$, $p_5=0$ and $p_6=-h/40$, when c is assumed to be a constant zero and

$$\alpha = \frac{ch}{2}\coth\left(\frac{ch}{2a}\right), \tag{2.5a}$$

$$p_1 = 90\beta^5-(12+90\gamma)\beta^4+(7.5+12\gamma)\beta^3-(0.5+\gamma)\beta+\frac{7}{30}+0.375\gamma, \tag{2.5b}$$

$$p_2 = 24\beta^4+\frac{8}{15}-24\beta^3\gamma+2\beta\gamma, \tag{2.5c}$$

$$p_3 = -90\beta^5-(12-90\gamma)\beta^4-(7.5-12\gamma)\beta^3+(0.5-\gamma)\beta+\frac{7}{30}-0.375\gamma, \tag{2.5d}$$

$$p_4 = h\left[30\beta^5-6\beta^4(1+5\gamma)+(3.5+6\gamma)\beta^3-(0.5+\gamma)\beta^2+\left(\frac{1}{30}+\frac{1}{24}\gamma\right)\right], \tag{2.5e}$$

$$p_5 = h\left(120\beta^5-120\beta^4\gamma+8\beta^3+2\beta^2\gamma-\frac{1}{3}\gamma\right), \tag{2.5f}$$

$$p_6 = h\left[30\beta^5+6\beta^4(1-5\gamma)+(3.5-6\gamma)\beta^3+(0.5-\gamma)\beta^2-\left(\frac{1}{30}-\frac{1}{24}\gamma\right)\right], \tag{2.5g}$$

for any non-zero constant c, where $\beta=a/ch$ and $\gamma=\alpha/ch$. However, c being not a constant makes the truncation error of the scheme (2.4), computed using Taylor series expansion, as $TE=-2K_2c_{xi}u_{xxi}-\{K_1c_{xi}+K_2c_{xxi}\}u_{xi}+\mathcal{O}(h^4)$, where $K_1=h(p_3-p_1)+(p_4+p_5+p_6)$ and $K_2=h^2(p_3+p_1)/2+h(p_6-p_4)$. Expanding K_1 and K_2 once again using Taylor series

expansion demonstrates that the scheme (2.4) is only of second order. Therefore, to incorporate the variable nature of c and also to improve the order of accuracy, the differential equation (2.3) is rewritten as

$$-Au_{xx}+Cu_x=f(x), \tag{2.6}$$

where

$$A=a-2K_2c_x \quad \text{and} \quad C=c+\{K_1c_x+K_2c_{xx}\}, \tag{2.7}$$

and then (2.6) is replaced with a difference equation

$$-\Lambda_i D_h^2 u_i+C_i D_h u_i=P_1f_{i-1}+P_2f_i+P_3f_{i+1}+P_4f_{x_i-1}+P_5f_{x_i}+P_6f_{x_i+1}, \tag{2.8}$$

where Λ and P_1-P_6 are some coefficients to be computed. Once again replacing f with $(-Au_{xx}+Cu_x)$ and making Eq. (2.8) exact for x, x^2, x^3, x^4, x^5, x^6 and e^{C_ix/A_i}, gives $\Lambda_i=A_i$, $P_1=2/15$, $P_2=11/15$, $P_3=2/15$, $P_4=h/40$, $P_5=0$ and $P_6=-h/40$, when $C_i=0$, and for $C_i\neq 0$,

$$\Lambda_i=\frac{C_ih}{2}\coth\left(\frac{C_ih}{2A_i}\right), \tag{2.9a}$$

$$P_1=90\overline{\beta}_i^{\,5}-(12+90\overline{\gamma}_i)\overline{\beta}_i^{\,4}+(7.5+12\overline{\gamma}_i)\overline{\beta}_i^{\,3}-(0.5+\overline{\gamma}_i)\overline{\beta}_i+\frac{7}{30}+0.375\overline{\gamma}_i, \tag{2.9b}$$

$$P_2=24\overline{\beta}_i^{\,4}+\frac{8}{15}-24\overline{\beta}_i^{\,3}\overline{\gamma}_i+2\overline{\beta}_i\overline{\gamma}_i, \tag{2.9c}$$

$$P_3=-90\overline{\beta}_i^{\,5}-(12-90\overline{\gamma}_i)\overline{\beta}_i^{\,4}-(7.5-12\overline{\gamma}_i)\overline{\beta}_i^{\,3}+(0.5-\overline{\gamma}_i)\overline{\beta}_i+\frac{7}{30}-0.375\overline{\gamma}_i, \tag{2.9d}$$

$$P_4=h\left[30\overline{\beta}_i^{\,5}-6\overline{\beta}_i^{\,4}(1+5\overline{\gamma}_i)+(3.5+6\overline{\gamma}_i)\overline{\beta}_i^{\,3}-(0.5+\overline{\gamma}_i)\overline{\beta}_i^{\,2}+\left(\frac{1}{30}+\frac{1}{24}\overline{\gamma}_i\right)\right], \tag{2.9e}$$

$$P_5=h\left(120\overline{\beta}_i^{\,5}-120\overline{\beta}_i^{\,4}\overline{\gamma}_i+8\overline{\beta}_i^{\,3}+2\overline{\beta}_i^{\,2}\overline{\gamma}_i-\frac{1}{3}\overline{\gamma}_i\right), \tag{2.9f}$$

$$P_6=h\left[30\overline{\beta}_i^{\,5}+6\overline{\beta}_i^{\,4}(1-5\overline{\gamma}_i)+(3.5-6\overline{\gamma}_i)\overline{\beta}_i^{\,3}+(0.5-\overline{\gamma}_i)\overline{\beta}_i^{\,2}-\left(\frac{1}{30}-\frac{1}{24}\overline{\gamma}_i\right)\right], \tag{2.9g}$$

where $\overline{\beta}_i=A_i/C_ih$, $\overline{\gamma}_i=\Lambda_i/C_ih$ and A and C are as defined in (2.7).

Scheme (2.8) produces a diagonally dominant tri-diagonal system of equations which can be solved efficiently using Thomas algorithm. The difference scheme (2.8) has derived from the modified equation (2.6) which may be a second order approximation to (2.6) but it is fourth order approximation to (2.3). To understand this, expand the RHS of (2.8) to obtain

$$f_i+\left[h(P_3-P_1)+(P_4+P_5+P_6)\right](f_x)_i+\left[\frac{h^2}{2}(P_3+P_1)+h(P_6-P_4)\right](f_{xx})_i+\mathcal{O}(h^4),$$

where the coefficients of $(f_x)_i$ and $(f_{xx})_i$ are equal up to fourth order if parameters P_1 to P_6 replaced by p_1 to p_6. Therefore the LHS of (2.8) will cancel the remainder terms obtained in (2.4), when c is variable type. Now the Taylor-series based truncation error analysis shows that (2.8) with (2.9) is a fourth order scheme for the CDE (2.3) with variable convection coefficients.

2.2 Two-dimensional case

Following the development of the scheme in one-dimensional case, when the convection coefficients are constant, the two-dimensional equivalent of (2.4) is

$$-\alpha_h D_h^2 u_{i,j} - \alpha_k D_k^2 u_{i,j} + cD_h u_{i,j} + dD_k u_{i,j} = F^*{}_{i,j}, \tag{2.10}$$

where

$$\begin{aligned} F^*{}_{i,j} &= p_1 f_{i-1,j} + p_2 f_{i,j} + p_3 f_{i+1,j} + p_4 f_{x_{i-1,j}} + p_5 f_{x_{i,j}} + p_6 f_{x_{i+1,j}} \\ &\quad + q_1 f_{i,j-1} + q_2 f_{i,j} + q_3 f_{i,j+1} + q_4 f_{y_{i,j-1}} + q_5 f_{y_{i,j}} + q_6 f_{y_{i,j+1}}, \\ \alpha_h &= \begin{cases} \frac{ch}{2}\coth(\frac{ch}{2a}), & c \neq 0, \\ a, & c = 0, \end{cases} \qquad \alpha_k = \begin{cases} \frac{dh}{2}\coth(\frac{dh}{2b}), & d \neq 0, \\ b, & d = 0, \end{cases} \end{aligned} \tag{2.11}$$

and the coefficients p_1 to p_6 are as given in (2.5). The coefficients q_1 to q_6 are equivalent to p_1 to p_6 of (2.5) but h, β and γ have to be replaced with k, b/dk and α_k/dk, respectively. The truncation error of the scheme (2.10), computed using Taylor series expansion, is given by

$$\begin{aligned} TE &= (K_1 d + L_1 c) u_{xy_{i,j}} + (L_2 c - K_1 b) u_{xyy_{i,j}} + (K_2 d - L_1 a) u_{xxy_{i,j}} \\ &\quad + (-K_2 b - L_2 a) u_{xxyy_{i,j}} + f_{i,j} + \mathcal{O}(h^4), \end{aligned} \tag{2.12}$$

where

$$K_1 = h(p_3 - p_1) + (p_4 + p_5 + p_6), \qquad K_2 = \frac{h^2}{2}(p_3 + p_1) + h(p_6 - p_4), \tag{2.13a}$$

$$L_1 = k(q_3 - q_1) + (q_4 + q_5 + q_6), \qquad L_2 = \frac{k^2}{2}(q_3 + q_1) + k(q_6 - q_4). \tag{2.13b}$$

Expanding the terms in (2.12) and (2.13) shows that the scheme (2.10) is of second order accurate. To make it fourth order, Eq. (2.10) is rewritten as

$$\left(-\alpha_h D_h{}^2 - \alpha_k D_k{}^2 + cD_h + dD_k + ED_h D_k + GD_k{}^2 D_h + HD_h{}^2 D_k + KD_h{}^2 D_k{}^2\right) u_{ij} = F_{ij}, \tag{2.14}$$

where α_h and α_k are same as in (2.11), p_1 to p_6 and q_1 to q_6 are exactly as in (2.10) and

$$E = K_1 d + L_1 c, \quad G = -K_1 b + L_2 c, \quad H = K_2 d - L_1 a, \quad K = -K_2 b - L_2 a, \tag{2.15a}$$

$$\begin{aligned} F_{i,j} &= p_1 f_{i-1,j} + p_2 f_{i,j} + p_3 f_{i+1,j} + p_4 f_{x_{i-1,j}} + p_5 f_{x_{i,j}} + p_6 f_{x_{i+1,j}} \\ &\quad + q_1 f_{i,j-1} + q_2 f_{i,j} + q_3 f_{i,j+1} + q_4 f_{y_{i,j-1}} + q_5 f_{y_{i,j}} + q_6 f_{y_{i,j+1}} - f_{i,j}. \end{aligned} \tag{2.15b}$$

To incorporate the variable nature of the convection coefficients c and d, the coefficients α_h, α_k, p_1 to p_6 and q_1 to q_6 in (2.14) are modified by replacing c, d, β, γ with c_{ij}, d_{ij}, β_{ij} and

γ_{ij}, respectively, and the modified values have been used in (2.13)-(2.15). The truncation error of the scheme (2.14), with variable convection coefficient is given by

$$\begin{aligned} TE=&(K_1c_x+K_2c_{xx}+L_1c_y+L_2c_{yy})u_x+(K_1d_x+K_2d_{xx}+L_1d_y+L_2d_{yy})u_y \\ &+2K_2c_xu_{xx}+2L_2d_yu_{yy}+(2K_2d_x+2L_2c_y)u_{xy}+\mathcal{O}(h^4). \end{aligned} \tag{2.16}$$

Since K_1, K_2, L_1 and L_2 are of second order, therefore, the scheme (2.14) is again only second order accurate. To make it $\mathcal{O}(h^4+k^4)$, the differential equation is further written as

$$-Au_{xx}-Bu_{yy}+Cu_x+Du_y=F_p, \tag{2.17}$$

where

$$A=a-2K_2c_x, \qquad B=b-2L_2d_y, \tag{2.18a}$$

$$C=c+K_1c_x+K_2c_{xx}+L_1c_y+L_2c_{yy}, \qquad D=d+K_1d_x+K_2d_{xx}+L_1d_y+L_2d_{yy}, \tag{2.18b}$$

$$F_p=f-2(K_2d_x+L_2c_y)u_{xy}. \tag{2.18c}$$

Now applying the finite difference scheme (2.14) to the modified differential equation (2.17) gives

$$\left(-\Lambda_h{D_h}^2-\Lambda_k{D_k}^2+CD_h+DD_k+\mathcal{E}D_hD_k+\mathcal{G}{D_k}^2D_h+\mathcal{H}{D_h}^2D_k+\mathcal{K}{D_h}^2{D_k}^2\right)u_{ij}=\mathcal{F}_{i,j}, \tag{2.19}$$

where

$$\Lambda_h=\begin{cases} \frac{C_{ij}h}{2}\coth(\frac{C_{ij}h}{2A_{ij}}), & C_{ij}\neq 0, \\ A_{ij}, & C_{ij}=0, \end{cases} \qquad \Lambda_k=\begin{cases} \frac{D_{ij}k}{2}\coth(\frac{D_{ij}k}{2B_{ij}}), & D_{ij}\neq 0, \\ B_{ij}, & D_{ij}=0, \end{cases} \tag{2.20}$$

and

$$\mathcal{E}=\mathcal{K}_1D_{ij}+\mathcal{L}_1C_{ij}+2(K_2d_{xij}+L_2c_{y_{ij}}), \qquad \mathcal{G}=-\mathcal{K}_1B_{ij}+\mathcal{L}_2C_{ij}, \tag{2.21a}$$

$$\mathcal{H}=\mathcal{K}_2D_{ij}-\mathcal{L}_1A_{ij}, \qquad \mathcal{K}=-\mathcal{K}_2B_{ij}-\mathcal{L}_2A_{ij}, \tag{2.21b}$$

$$\begin{aligned} \mathcal{F}_{i,j}=&P_1f_{i-1,j}+P_2f_{i,j}+P_3f_{i+1,j}+P_4f_{x_{i-1,j}}+P_5f_{x_{i,j}}+P_6f_{x_{i+1,j}} \\ &+Q_1f_{i,j-1}+Q_2f_{i,j}+Q_3f_{i,j+1}+Q_4f_{y_{i,j-1}}+Q_5f_{y_{i,j}}+Q_6f_{y_{i,j+1}}-f_{i,j}, \end{aligned} \tag{2.21c}$$

and $\mathcal{K}_1$,$\mathcal{K}_2$,$\mathcal{L}_1$ and $\mathcal{L}_2$ are defined as

$$\mathcal{K}_1=h(P_3-P_1)+(P_4+P_5+P_6), \qquad \mathcal{K}_2=\frac{h^2}{2}(P_3+P_1)+h(P_6-P_4), \tag{2.22a}$$

$$\mathcal{L}_1=k(Q_3-Q_1)+(Q_4+Q_5+Q_6), \qquad \mathcal{L}_2=\frac{k^2}{2}(Q_3+Q_1)+k(Q_6-Q_4), \tag{2.22b}$$

with

$$P_1=90{\beta_{ij}}^5-(12+90\gamma_{ij}){\beta_{ij}}^4+(7.5+12\gamma_{ij}){\beta_{ij}}^3-(0.5+\gamma_{ij})\beta_{ij}+\frac{7}{30}+0.375\gamma_{ij}, \tag{2.23a}$$

$$P_2 = 24{\beta_{ij}}^4 + \frac{8}{15} - 24{\beta_{ij}}^3\gamma_{ij} + 2\beta_{ij}\gamma_{ij}, \tag{2.23b}$$

$$P_3 = -90{\beta_{ij}}^5 - (12-90\gamma_{ij}){\beta_{ij}}^4 - (7.5-12\gamma_{ij}){\beta_{ij}}^3 + (0.5-\gamma_{ij})\beta_{ij} + \frac{7}{30} - 0.375\gamma_{ij}, \tag{2.23c}$$

$$P_4 = h\Big[30{\beta_{ij}}^5 - 6{\beta_{ij}}^4(1+5\gamma_{ij}) + (3.5+6\gamma_{ij}){\beta_{ij}}^3 - (0.5+\gamma_{ij}){\beta_{ij}}^2 + \Big(\frac{1}{30} + \frac{1}{24}\gamma_{ij}\Big)\Big], \tag{2.23d}$$

$$P_5 = h\Big(120{\beta_{ij}}^5 - 120{\beta_{ij}}^4\gamma_{ij} + 8{\beta_{ij}}^3 + 2{\beta_{ij}}^2\gamma_{ij} - \frac{1}{3}\gamma_{ij}\Big), \tag{2.23e}$$

$$P_6 = h\Big[30{\beta_{ij}}^5 + 6{\beta_{ij}}^4(1-5\gamma_{ij}) + (3.5-6\gamma_{ij}){\beta_{ij}}^3 + (0.5-\gamma_{ij}){\beta_{ij}}^2 - \Big(\frac{1}{30} - \frac{1}{24}\gamma_{ij}\Big)\Big], \tag{2.23f}$$

where $\beta_{ij} = A_{ij}/C_{ij}k$ and $\gamma_{ij} = \Lambda_h/C_{ij}k$, similarly Q_1 and Q_2 are obtained by replacing $\beta_{ij} = B_{ij}/D_{ij}k$ and $\gamma_{ij} = \Lambda_k/D_{ij}k$ in P_1 to P_6. Finally, the Taylor series based truncation error analysis shows that the scheme (2.19) is $\mathcal{O}(h^4+k^4)$. Scheme (2.19) with (2.20), (2.21) and (2.22) is solved using SLOR over a nine point stencil. The tri-diagonal system in SLOR is solved using Thomas algorithm.

3 Nonlinear models

If c and d are also functions of the unknown u, the coefficients in (2.19) contains u and its partial derivatives, therefore, an iterative procedure is required to compute the solution. In the present model, an initial approximation which satisfies the boundary conditions is assumed for the unknown and (2.19) is solved using SLOR procedure until convergence. The first and second partial derivatives of the convection coefficients required in the algorithm are computed at the beginning of the every iteration using the following fourth order Padé scheme [3,9]

$$f'_{i-1} + 4f'_i + f'_{i+1} = \frac{3}{h}(f_{i+1} - f_{i-1}), \tag{3.1a}$$

$$f''_{i-1} + 10f''_i + f''_{i+1} = \frac{12}{h^2}(f_{i+1} - f_{i-1}), \tag{3.1b}$$

for $i = 2,\cdots,N-1$, with third order boundary closures

$$f'_1 + 2f'_2 = \frac{1}{2h}(-5f_1 + 4f_2 + f_3), \tag{3.2a}$$

$$f'_{N-1} + 2f'_N = -\frac{1}{2h}(-5f_{N-2} + 4f_{N-1} + f_N), \tag{3.2b}$$

$$f''_1 + 11f''_2 = \frac{1}{h^2}(13f_1 - 27f_2 + 15f_3), \tag{3.2c}$$

$$f''_{N-1} + 11f''_N = \frac{1}{h^2}(13f_{N-2} - 27f_{N-1} + 15f_N), \tag{3.2d}$$

where f is either c or d and the prime is the partial derivative with respect to x or y. The final algorithm for the nonlinear model is as follows.

Algorithm 3.1: Algorithm for the nonlinear model

Step 1: Initialize u.
Step 2: Compute c_x, c_y, c_{xx}, c_{yy}, d_x, d_y, d_{xx} and d_{yy} using (3.1) and (3.2).
Step 3: Compute α_h, α_k, p_1 to p_6 and q_1 to q_6.
Step 4: Compute $K1$, $K2$, $L1$ and $L2$ using (2.13).
Step 5: Compute E, G, H and K using (2.15).
Step 6: Compute A, B, C and D using (2.18).
Step 7: Compute Λ_h, Λ_k, P_1 to P_6 and Q_1 to Q_6.
Step 8: Compute $\mathcal{K}_1$, $\mathcal{K}_2$, $\mathcal{L}_1$ and $\mathcal{L}_2$ using (2.22).
Step 9: Compute $\mathcal{E}$, $\mathcal{G}$ and $\mathcal{H}$ and $\mathcal{K}$ using (2.21).
Step 10: Solve the difference system (2.19) using SLOR.
Step 11: Update the solution u.
Step 12: Repeat Steps 2 to 10 until convergence.

The convergence of the above iterative procedure and the spectral resolution of the developed scheme will be discussed in the next section.

4 Mathematical analysis

4.1 Convergence of the iterative procedure

The fourth order compact exponential scheme (2.8) can be rewritten as

$$\frac{C_i}{2h}\Big[-\Big(\coth\Big(\frac{C_ih}{2A_i}\Big)+1\Big)u_{i-1}+2\coth\Big(\frac{C_ih}{2A_i}\Big)u_i-\Big(\coth\Big(\frac{C_ih}{2A_i}\Big)-1\Big)u_{i+1}\Big]=F_i,$$

where

$$F_i=P_1f_{i-1}+P_2f_i+P_3f_{i+1}+P_4f_{x_i}+P_5f_{x_i}+P_6f_{x_{i+1}}.$$

Since $|\coth(C_ih/2A_i)|\geq 1$, the off diagonal elements of coefficient matrix $A=(a_{ij})$ are of same sign and diagonal elements are of opposite sign. Further, matrix A has all real entries and is irreducible diagonally dominant. Therefore A is an M-matrix (A^{-1} exists with $A^{-1}>0$), which guarantees the convergence of the iterative process.

4.2 Wave number analysis

Scheme (2.8) is a fourth order exponential HOC scheme to the differential equation (2.3) in which the coefficients are functions of A and C. For the sake of simplicity the wave

number analysis has been carried on an equivalent scheme given by

$$\begin{aligned}&-(\alpha_i-2K_2c_x)D_h^2u_i+(c_i+k_1c_x+k_2c_{xx})D_hu_i\\&=p_1f_{i-1}+p_2f_i+p_3f_{i+1}+p_4f_{x_{i-1}}+p_5f_{x_i}+p_6f_{x_{i+1}},\end{aligned}\tag{4.1}$$

where the coefficients p_1 to p_6 are same as in (2.5) and $\beta=a/c_ih$ and $\gamma=\alpha/c_ih$. Expanding the RHS and LHS of (2.8) and (4.1) one can see that both schemes are equal up to fourth order. Therefore, with respect to accuracy and the discrete source term both difference schemes are equivalent. However, in the computations (2.8) has to be used because it guarantees the M-matrix.

To verify the wave resolution of any numerical scheme, the characteristic graphs of the difference equation and the differential equation are compared for various Peclet numbers defined by $p=ch/a$. Due to the variable nature of the convection coefficients, the value of the Peclet number can vary from point to point and hence analysis is based on the maximum cell Peclet number defined by $p_e=c^*h/a$, where $c^*=\sup_{x\in[r_0,r_1]}\{|C(x)|\}$. The characteristic of the differential equation is obtained by substituting e^{Ikx} at u which gives

$$\lambda=\frac{\phi^2}{p_e}+I\phi,\tag{4.2}$$

where $\phi=kh$, k is the wave number, $I=\sqrt{-1}$. Similarly, the characteristic of the developed difference scheme (2.8) is obtained by substituting e^{Iikh} at u_i. Now the characteristic for Eq. (4.1)

$$\lambda^*=\frac{\gamma k''+Ik'+(-2\kappa_2k''+I\kappa_1k')\mu_1+I\kappa_2k'\mu_2}{z^2+iz^1},\tag{4.3}$$

where

$$\begin{aligned}&k'=\sin\phi,\quad k''=2-2\cos\phi,\quad \gamma=\frac{1}{2}\Big(\coth\frac{p_e}{2}\Big),\quad \mu_1=\frac{hc_x}{a},\quad \mu_2=\frac{h^2c_{xx}}{a},\\&\kappa_2=\frac{1}{2}(\nu_3+\nu_1)+(\nu_6-\nu_4),\qquad \kappa_1=(\nu_3-\nu_1)+(\nu_4+\nu_5+\nu_6),\\&z^1=\big[(\nu_3-\nu_1)\sin\phi+\phi(\nu_5+(\nu_6+\nu_4)\cos\phi)\big],\\&z^2=\big[\nu_2+(\nu_3+\nu_1)\cos\phi-\phi(\nu_6-\nu_4)\sin\phi\big],\\&\nu_1=\frac{1}{p_e^5}\Big[90-(12+90\gamma)p_e+(7.5+12\gamma)p_e^2-(0.5+\gamma)p_e^4+\Big(\frac{7}{30}+0.375\gamma\Big)p_e^5\Big],\\&\nu_2=\frac{1}{p_e^4}\Big(\frac{8}{15}p_e^4+2\gamma p_e^3-24p_e^2+24\gamma\Big),\\&\nu_3=\frac{1}{p_e^5}\Big[-90-(12-90\gamma)p_e-(7.5-12\gamma)p_e^2+(0.5-\gamma)p_e^4+\Big(\frac{7}{30}-0.375\gamma\Big)p_e^5\Big],\\&\nu_4=\frac{1}{p_e^5}\Big[30-6(1+5\gamma)p_e+(3.5+6\gamma){p_e}^2-(0.5+\gamma){p_e}^3+\Big(\frac{1}{30}+5\gamma\Big){p_e}^5\Big],\\&\nu_5=\frac{1}{p_e^5}\Big(120-120\gamma p_e+8Pe^2+2\gamma{p_e}^3-\gamma p_e^5\Big),\end{aligned}$$

$$\nu_6 = \frac{1}{p_e^5}\left[30+6(1-5\gamma)p_e+(3.5-6\gamma){p_e}^2+(0.5-\gamma){p_e}^3-\left(\frac{1}{30}-5\gamma\right){p_e}^5\right].$$

Similarly the characteristic of the existing scheme [15] given by

$$\lambda_{[15]} = \frac{\gamma k''+Ik'+(-2\psi_2 k''+I\psi_1 k')\mu_1+I\psi_2 k'\mu_2}{i\psi_1 k'+(1-\psi_2 k'')}, \tag{4.4}$$

where $\psi_1=(1-p_e\gamma)/p_e$ and $\psi_2=(1-p_e\gamma)/{p_e}^2+1/6$, and

$$\lambda_{[10]} = \frac{\gamma k''+Ik'+(-k''/6+Ik' p_e/12)\mu_1+Ik'\mu_2/12}{i(\eta_3-\eta_1)\sin\phi+\eta_2+(\eta_1+\eta_3)\cos\phi}, \tag{4.5}$$

where $\eta_1 = 1/6+(1-p_e\gamma)(2-p_e)/2p_e^2$, $\eta_2 = 2/3+2(1-p_e\gamma)/p_e^2$, and $\eta_3 = 1/6+(1-p_e\gamma)(2+p_e)/2p_e^2$, and k', k'', γ, p_e, μ_1 and μ_2 are same as in (4.3). Its clear from (4.3) that if the parameters μ_1 and μ_2 are zero, then the characteristics are the same as the constant coefficients case as given in [13]. For non-zero case they can be made $|\mu_1|=|\mu_2|\leq r$, by fixing the step length

$$h \leq \min\left\{\frac{r}{||\frac{c_{xx}}{c}||_\infty}, \sqrt{\frac{r}{||\frac{c_{xx}}{c}||_\infty}}\right\}.$$

Fixing $r=0.01$ the real and imaginary parts of characteristics of different schemes are plotted for various Peclet numbers in Figs. 1 and 2, respectively. In these comparisons the characteristics given in (4.3), (4.4) and (4.5) are plotted against the characteristic (4.2) obtained form the differential operator. In all the comparisons, the developed scheme agrees with the (4.2) much better than any of the existing exponential schemes for both real and imaginary parts of the characteristic for both $Pe=2$ and 10. The characteristic of (4.5) appears to be better than (4.4) due to its overshoot nature, however quantitatively they are same. The comparisons can be made quantitative in the following way.

4.2.1 Resolving efficiency

The resolving efficiency [7] of any numerical scheme, defined by $\phi_{\max}/\pi$, is a number between 0 and 1, where $\phi_{\max}$, independent of the grid size, is the maximum value of ϕ for which $|\lambda_{fd}-\lambda_{exact}|$ is less than a tolerance δ. Resolving efficiencies are computed for various schemes with $\delta=0.01$ and $|\mu_1|=|\mu_2|=0.01$ and presented in Table 1. The comparisons made in this table quantify the superiority of the developed scheme over

Table 1: Resolving efficiency of the real and imaginary parts of λ.

	Pe for $Im(\lambda)$				Pe for $Re(\lambda)$			
Scheme	0.1	2.0	10.0	100.0	0.1	2.0	10.0	100.0
Present	0.59	0.57	0.53	0.50	0.41	0.59	0.71	0.67
Ref. [15]	0.32	0.35	0.34	0.28	0.27	0.30	0.24	0.22
Ref. [10]	0.30	0.31	0.44	0.04	0.25	0.30	0.23	0.15

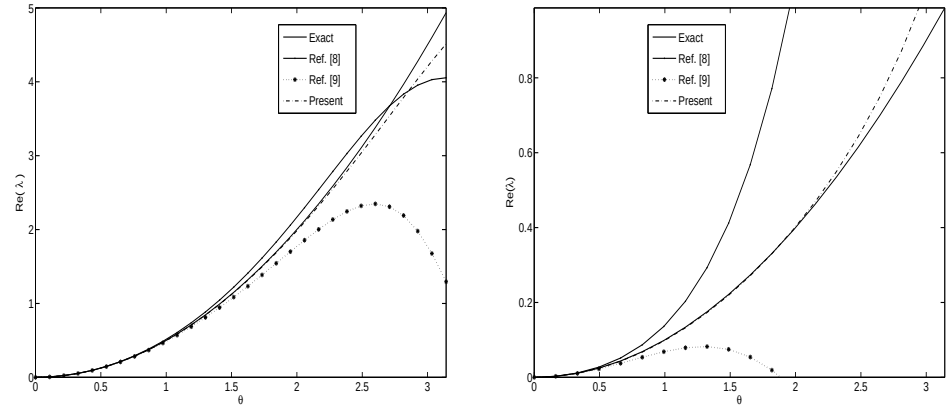

Figure 1: Real characteristic for $Pe=2,10$.

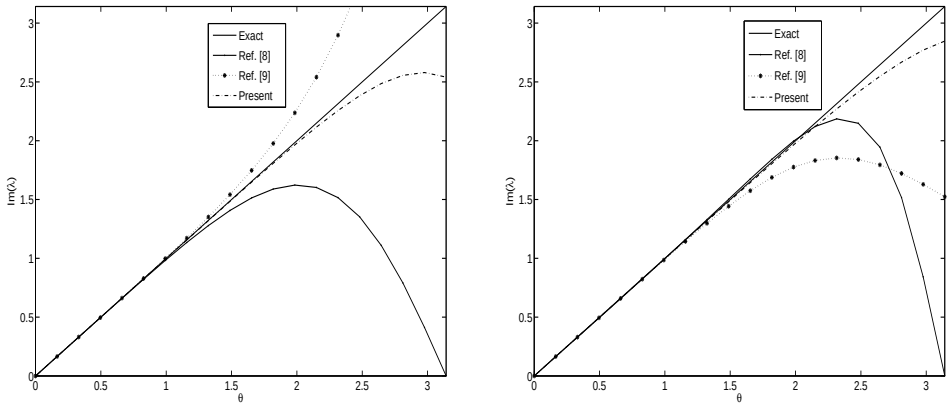

Figure 2: Imaginary characteristic for $Pe=2,10$.

some of the existing exponential schemes. Though order of all these schemes is same (fourth order), the better resolution of the developed scheme can help in generating more accurate solutions.

5 Numerical validation

The developed scheme has been validated for variable and nonlinear CDE separately. In both the cases, the error norms and rates of convergence have been compared with the existing results. For all the chosen problems, the diffusion parameter has been taken as 1.0, 0.1 and 0.01. The grid sizes have been varied as 41, 81, 161, 321 and 641 for all the one-dimensional CDE and 11×11, 21×21, 41×41, 81×81 and 101×101 for all the two-dimensional problems. To demonstrate the observations made in the wave number anal-

ysis, the comparisons are also made with respect to Peclet number. In every case, the error norms based on infinity norm have been computed to highlight the maximum error which is in-general expected in the boundary layer regions. The rate of convergence is computed using

$$rate = \frac{\log\left(\frac{E^h}{E^{h/2}}\right)}{\log(2)}, \tag{5.1}$$

where E^h and $E^{h/2}$ are the error norms with the grid sizes h and $h/2$, respectively.

5.1 Variable convection problems

In this case the convection coefficients are functions of x and y, however, they are assumed to be known. Three model problems, two for one-dimensional and one problem for two-dimension, have been chosen with variable convection coefficients to validate the developed scheme. The chosen problems have a sharp boundary layer with respect to the diffusion coefficient. In all the one-dimensional problems, the resulting tri-diagonal system of equations is solved using Thomas algorithm. SLOR based iterative schemes has been used in the two-dimensional problems.

Example 5.1.

$$-\epsilon u_{xx} + (2-x)u_x + u = f(x), \quad 0 < \epsilon \leq 1, \quad 0 < x < 1,$$

with the exact solution

$$u(x) = \sin^2(\pi x) + xe^{\frac{x-1}{\epsilon}}.$$

Example 5.2.

$$-\epsilon u_{xx} + \left(\frac{x+2}{x+1}\right)u_x = f(x), \quad 0 < \epsilon \leq 1, \quad 0 < x < 1,$$

with the exact solution

$$u(x) = \frac{(x+1)^{1+\frac{1}{\epsilon}} - 1}{2^{1+\frac{1}{\epsilon}} - 1}.$$

Due to the high gradients of the solution in the boundary layer region, computing the solution accurately is very challenging for any numerical scheme. Error norms based on infinity norm indicates the robustness of the numerical schemes, therefore, the error norms and rates of convergence have been presented in Table 2 for Example 5.1. For all the three chosen $\epsilon = 0.01, 0.1, 1$, the grid density has been varied from a course 21 to a very fine 321 and in every case an improved accuracy and fourth order rate has been demonstrated. Its clear from these comparisons that the present scheme consistently generated fourth order rate and higher order of accuracy. The comparisons for Example 5.2, given in Table 3, are made with respect to Peclet number to demonstrate the observations made in the wave number analysis. This Peclet number based comparisons show that the developed solutions are better by an order over the existing schemes at high Peclet number like 10 and becomes better by three orders when the Peclet number is reduced to one.

Table 2: Comparison of the error and convergence rate for Example 5.1.

		Present		Ref. [15]		Ref. [10]	
ϵ	No. nodes	Max Error	Rate	Max Error	Rate	Max Error	Rate
1.0	21	6.74807(-07)	–	2.76500(-05)	–	4.27913(-05)	–
	41	3.86295(-08)	3.9678	1.73075(-06)	3.9978	2.68254(-06)	3.9956
	81	2.35823(-09)	4.0085	1.08066(-07)	4.0014	1.67581(-07)	4.0007
	161	1.46525(-10)	4.0339	6.75245(-09)	4.0004	1.04726(-08)	4.0002
	321	9.36477(-12)	4.1267	4.22002(-10)	4.0001	6.54553(-10)	4.0000
0.1	21	1.50062(-05)	–	5.27315(-05)	–	7.94336(-05)	–
	41	9.19222(-07)	4.0290	3.36368(-06)	3.9706	5.13242(-06)	3.9520
	81	5.73204(-08)	4.0033	2.11295(-07)	3.9927	3.2351(-07)	3.9878
	161	3.58201(-09)	4.0002	1.32255(-08)	3.9979	2.02676(-08)	3.9966
	321	2.23837(-10)	4.0002	8.26910(-10)	3.9994	1.26732(-09)	3.9993
0.01	21	4.19183(-03)	–	1.32144(-03)	–	9.65440(-03)	–
	41	6.47709(-04)	2.6942	3.17139(-04)	2.0589	1.15974(-03)	3.0574
	81	5.44838(-05)	3.5714	1.74053(-05)	4.1875	9.48679(-05)	3.6117
	161	3.13560(-06)	4.1190	1.12582(-06)	3.9505	6.43208(-06)	3.8826
	321	1.97880(-07)	3.9860	6.92626(-08)	4.0228	4.10723(-07)	3.9690

Table 3: Comparison of the error norm for Example 5.2.

			Present	Ref. [15]	Ref. [10]
Pe	$\frac{1}{h}$	$\frac{1}{\epsilon}$	Max Error	Max Error	Max Error
1	10	5	1.52470(-05)	3.08950(-05)	4.87470(-05)
	40	20	2.23288(-06)	2.39153(-05)	3.50760(-05)
	100	50	8.15199(-07)	2.19682(-05)	3.26601(-05)
	1000	500	6.93955(-08)	2.08919(-05)	3.13925(-05)
5	10	25	4.59570(-04)	9.61674(-03)	1.55513(-02)
	40	100	1.28263(-05)	8.90269(-03)	1.44025(-02)
	100	250	6.91681(-05)	8.76492(-03)	1.41957(-02)
8	10	40	4.32314(-04)	2.91651(-02)	5.42063(-02)
	40	160	1.15165(-03)	2.80492(-02)	5.17008(-02)
	100	400	1.28921(-03)	2.78254(-02)	5.12329(-02)
10	10	50	2.91566(-03)	4.15582(-02)	8.76718(-02)
	40	200	3.72308(-03)	4.05919(-02)	8.45360(-02)
	100	500	3.87916(-03)	4.03921(-02)	8.39433(-02)

Example 5.3. Consider the following two-dimensional CDE in the domain $\Omega = [0,1] \times [0,1]$:

$$-\epsilon u_{xx} - \epsilon u_{yy} + x u_x = f(x,y),$$

with the exact solution

$$u(x,y) = \frac{(1-y)y - 2x\epsilon}{e^{\frac{x}{\epsilon}}}.$$

Table 4: Comparison of the error and convergence rate for Example 5.3.

		Present		Ref. [15]		Ref. [10]	
ϵ	No. nodes	Max Error	Rate	Max Error	Rate	Max Error	Rate
0.1	11×11	1.66566(-04)	–	2.51255(-04)	–	8.74422(-04)	–
	21×21	1.12219(-05)	3.8917	1.63431(-05)	3.9424	5.57114(-05)	3.9723
	41×41	7.14868(-07)	3.9725	1.02962(-06)	3.9885	3.49417(-06)	3.9950
	81×81	4.50340(-08)	3.9886	6.45400(-08)	3.9958	2.18707(-07)	3.9979
0.05	11×11	2.21998(-04)	–	5.85841(-03)	–	1.24713(-02)	–
	21×21	5.35730(-05)	2.0510	4.37602(-04)	3.7428	8.55985(-04)	3.8649
	41×41	4.11448(-06)	3.7027	2.84571(-05)	3.9428	5.45281(-05)	3.9725
	81×81	2.68957(-07)	3.9353	1.79634(-06)	3.9857	3.42438(-06)	3.9931
0.01	11×11	2.36814(-00)	–	2.23448(-01)	–	1.92745(-00)	–
	21×21	1.41743(-01)	4.0624	1.14270(-01)	0.9675	3.17309(-01)	2.6027
	41×41	3.81177(-03)	5.2167	1.76305(-02)	2.6963	3.17442(-02)	3.3213
	81×81	5.70041(-05)	6.0633	1.44833(-03)	3.6056	2.31373(-03)	3.7782

Example 5.3, has been solved using the two-dimensional model of the scheme and the results are presented in Table 4. These comparisons show that the present scheme out performs the existing schemes and even produces a sixth order rate in some cases (say at $\epsilon=0.01$ with 81×81 nodes for Example 5.3 in the Table 4). It can also be observed that the rate of convergence for [15] goes below four at $\epsilon=0.01$. Further, the accuracy of the present scheme improved by an order over [10] and also [15] when grid densities are increased to 81×81. One interesting observation of the developed scheme, may be due to its better spectral resolution, is its better accuracy over the existing schemes at small diffusion parameters, wherein, in-general numerical schemes are known to be less accurate due to the existence of sharp boundary layers. To highlight the performance of the developed scheme, the analytical and obtained numerical solutions of the present scheme and [15] for Example 5.3 are compared in Fig. 3. In this figure the solutions obtained at $y=0.125$ and $y=0.5$ with diffusion parameter $\epsilon=0.01$ and grid density $N=81\times81$ are compared with the analytical solution in the boundary layer region that is in the window $0\leq x\leq 0.2$. The comparison shows that the solutions obtained using the present scheme and [15] are both very accurate even in the boundary layer region. However, to establish the better performance of the developed scheme over [15], the absolute errors at $y=0.125$, $y=0.25$ and $y=0.5$ with diffusion parameter $\epsilon=0.01$ for the same problem are compared in Fig. 4. Its clear from this comparison that the solution obtained using the present is at least an order better over the corresponding solution obtained using [15] at all the three constant y locations.

5.2 Nonlinear convection problems

In this case the convection coefficients are functions of x, y and also the unknown u and its partial derivatives. Once again one-dimensional and two-dimensional example prob-

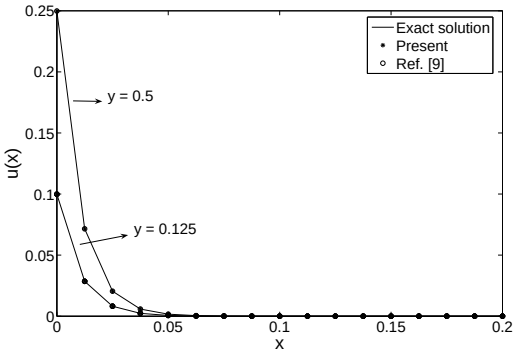

Figure 3: Comparison of the exact and numerical solutions for Example 5.3 with $\epsilon = 0.01$ and $N = 81 \times 81$.

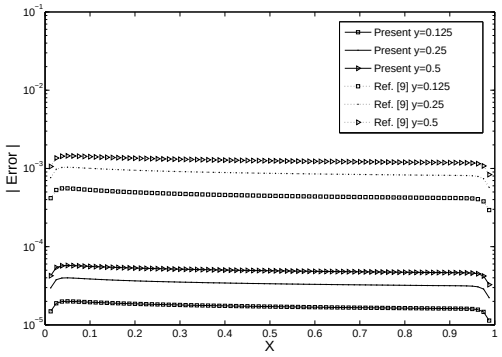

Figure 4: Comparison of the absolute error for Example 5.3 with $\epsilon = 0.01$ at various y locations.

lems have been solved iteratively, and the results have been compared. As already been mentioned, the required partial derivatives of the convection coefficients are computed numerically using fourth-order Padé schemes (3.1) and (3.2) for every iteration.

Example 5.4.

$$-\epsilon u_{xx} + u u_x = f(x), \quad 0 < \epsilon \leq 1, \quad 0 < x < 1,$$

with the exact solution

$$u(x) = \log\left(1 + x/\epsilon\right) + \cos(\pi x).$$

Example 5.5.

$$-\epsilon u_{xx} + u u_x = f(x), \quad 0 < \epsilon \leq 1, \quad 0 < x < 1,$$

with the exact solution

$$u(x) = e^{-x} + e^{(x-1)(1+\epsilon)/\epsilon}.$$

Examples 5.4 and 5.5 have sharp boundary layers. The error norms and rates of convergence for these test problems have been presented in Tables 5 and 6, respectively. Once again a consistent fourth order rate of convergence is realized even for small diffusion parameter and the additionally added iterative procedure did not affect either the order of accuracy or the rate of convergence.

Example 5.6. Consider the nonlinear CDE

$$-\epsilon u_{xx} - \epsilon u_{yy} + u u_y = f(x,y), \quad \text{for } (x,y) \in \Omega = [0,1] \times [0,1],$$

with the exact solution

$$u(x,y) = e^{y-x} + 2^{-\frac{1}{\epsilon}} (1+x)^{1+\frac{1}{\epsilon}}.$$

Example 5.7. Consider the nonlinear CDE

$$-\epsilon u_{xx} - \epsilon u_{yy} + u u_x = f(x,y), \quad \text{for } (x,y) \in \Omega = [0,1] \times [0,1],$$

with the exact solution

$$u(x,y) = \log\left(1 + x/\epsilon\right) + e^{y}.$$

Table 5: Comparison of the error and convergence rate for Example 5.4.

		Present		Ref. [15]		Ref. [10]	
ϵ	No. nodes	Max Error	Rate	Max Error	Rate	Max Error	Rate
0.1	41	1.27619(-05)	–	7.38332(-05)	–	9.77570(-05)	–
	81	8.42617(-07)	3.9208	4.96057(-06)	3.8957	6.36558(-06)	3.9408
	161	5.33543(-08)	3.9812	3.15913(-07)	3.9729	4.02179(-07)	3.9844
	321	3.43849(-09)	3.9558	1.98192(-08)	3.9946	2.52051(-08)	3.9961
	641	2.08565(-10)	4.0432	1.22690(-09)	4.0138	1.57642(-09)	3.9990
0.05	41	8.48229(-05)	–	6.72396(-04)	–	1.17888(-03)	–
	81	6.20280(-06)	3.7735	5.31901(-05)	3.6601	8.34374(-05)	3.8206
	161	4.24499(-07)	3.8691	3.57722(-06)	3.8942	5.40717(-06)	3.9477
	321	2.70746(-08)	3.9707	2.27919(-07)	3.9722	3.41167(-07)	3.9863
	641	1.49606(-09)	4.1777	1.43526(-08)	3.9891	2.13742(-08)	3.9965
0.01	41	2.47369(-02)	–	3.55143(-02)	–	1.62986(-01)	–
	81	2.04255(-03)	3.5982	9.05132(-03)	1.9722	2.46946(-02)	2.7225
	161	1.83259(-04)	3.4784	1.32309(-04)	2.7742	2.47913(-03)	3.3163
	321	1.38247(-05)	3.7286	1.16707(-05)	3.5029	1.86219(-04)	3.7348
	641	9.76648(-07)	3.8233	8.22033(-07)	3.8276	1.23596(-05)	3.9133

Table 6: Comparison of the error and convergence rate for Example 5.5.

		Present		Ref. [15]		Ref. [10]	
ϵ	No. nodes	Max Error	Rate	Max Error	Rate	Max Error	Rate
0.1	41	2.75431(-06)	–	5.53907(-06)	–	7.16300(-06)	–
	81	1.83801(-07)	3.9055	3.42264(-07)	4.0165	4.73373(-07)	3.9195
	161	1.16412(-08)	3.9808	2.15164(-08)	3.9916	2.98327(-08)	3.9880
	321	8.36666(-10)	3.9737	1.45497(-09)	3.8864	1.87223(-09)	3.9941
	641	4.54854(-11)	4.2012	2.02681(-10)	2.8437	1.17124(-10)	3.9986
0.05	41	2.50371(-05)	–	8.94949(-05)	–	1.01332(-04)	–
	81	1.73472(-06)	3.8513	5.00705(-06)	4.1598	7.13386(-06)	3.8283
	161	1.16043(-07)	3.9020	3.10486(-07)	4.0114	4.62292(-07)	3.9478
	321	7.02111(-09)	4.0468	1.95295(-08)	3.9908	2.92675(-08)	3.9814
	641	3.48593(-10)	4.3321	1.32661(-09)	3.8798	1.83245(-09)	3.9975
0.01	41	7.75110(-02)	–	2.96140(-02)	–	9.19937(-03)	–
	81	2.80512(-03)	4.7883	3.90138(-03)	2.9242	5.66382(-04)	4.0217
	161	8.72474(-05)	5.0068	2.17516(-04)	4.1648	2.17276(-04)	1.3822
	321	4.43131(-06)	4.2299	1.12092(-05)	4.2784	1.63308(-05)	3.7339
	641	2.25883(-07)	4.2941	7.00104(-07)	4.0010	1.10912(-06)	3.8801

For Examples 5.6 and 5.7, the rate of convergence is given in Figs. 5(a) and 5(b), respectively. In these figures, power law graphs $y = cx^d$ have been drawn for the mean error y computed over different grid densities x. The negative sign of d in this figure represent the decrease of mean error with the increase of grid density and the magnitude of d represents the rate of convergence. The value of d close to five in the present case

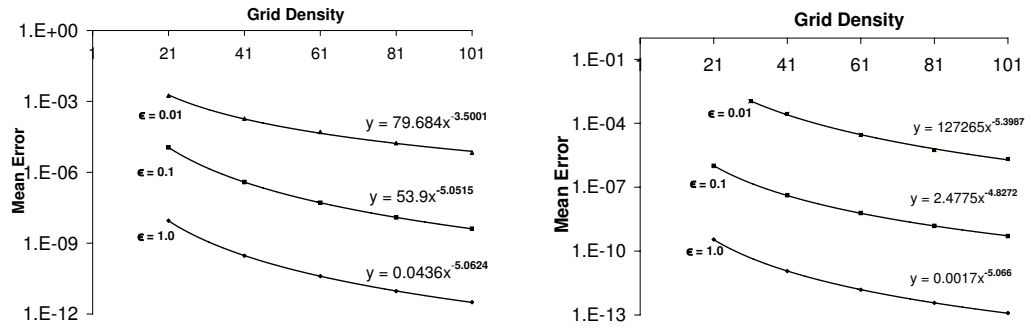

Figure 5: Accuracy and rate of convergence for (a) Example 5.6, (b) Example 5.7.

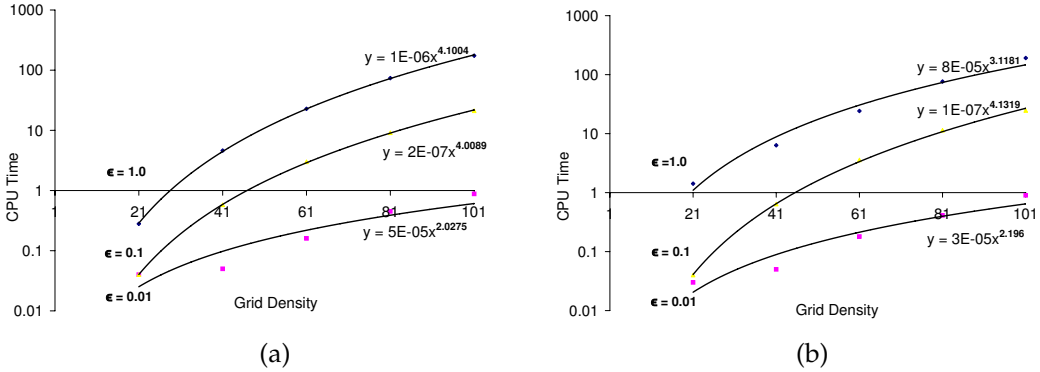

Figure 6: Comparison of the CPU times for (a) Example 5.6, (b) Example 5.7.

again conforms the robustness of the developed scheme.

It is observed in these numerical experiments that the iterative procedure for the nonlinear model of the developed scheme requires under relaxation for large grid densities and particularly for high diffusion parameters. For small diffusion parameters, the iterative procedure converged in less than a second even over a 101×101 grid. To demonstrate the computational time requirement of the scheme, the CPU times computed on a HP DL 140 server have been compared in the Figs. 6(a) and 6(b) for different grid densities for Examples 5.6 and 5.7. In these graphs, the x-coordinate, say 21, must be read as a 21×21 grid. It is also clear from the power law graph that for large diffusion parameter say at $\epsilon=1$, the increase in the computational time is four times with the increase in the grid density, however at low diffusion parameter its only quadratic increment. For a quantitative comparison, the CPU times required by the developed scheme and [15] are compared in Table 7 for Examples 5.6 and 5.7. In these comparisons, the CPU time requirements of the problems with the diffusion parameter $\epsilon=1,0.1,0.01$ and the grid densities $N=21,41,61,81,$and101 are included. It is once again very clear from these comparisons that the developed scheme requires a much smaller computational times, for all the chosen cases, over [15].

Table 7: Comparison of CPU time for the 2D non-linear problems.

	Example 5.6						Example 5.7					
	Present			Ref. [15]			Present			Ref. [15]		
# Nodes / ϵ	1.0	0.1	0.01	1.0	0.1	0.01	1.0	0.1	0.01	0.1	0.1	0.01
21×21	0.28	0.04	0.04	0.4	0.38	0.05	1.42	0.04		0.4	0.09	
41×41	4.61	0.58	0.05	6.23	6.26	0.48	6.33	0.64	0.09	6.1	1.48	0.17
61×61	22.76	3.00	0.16	30.16	29.99	2.50	24.23	3.58	0.18	30.3	8.59	0.48
81×81	73.73	9.13	0.45	93.96	94.43	8.33	76.52	11.4	0.64	157.21	26.92	1.16
101×101	174.23	21.18	0.88	219.77	224.77	20.29	191.38	24.64	0.90	376.45	51.91	2.02

Table 8: Comparison of mean error, convergence rate and CPU times for Example 5.7 with $\epsilon = 0.01$ when the partial derivatives of the convection coefficients are approximated using Central Difference (CD) and Padé scheme.

	CD			Padé		
No. nodes	Mean Error	Rate	CPU	Mean Error	Rate	CPU
41×41	3.14(-03)	–	0.08	2.76(-04)	–	0.09
81×81	5.80(-04)	2.43	0.52	5.53(-06)	5.64	0.64
161×161	9.13(-05)	2.68	6.37	3.34(-07)	4.05	8.40

Since coefficients of the partial derivatives of convection coefficients in (2.18) and (2.21) are second order accurate, therefore, it is sufficient to use second order approximations to discretize the partial derivatives of the convection coefficients. However such an approximation has produced third order rate as shown in Table 8 for Example 5.7 with ϵ=0.01. By replacing these second order approximations with fourth order Padé as given in (3.1) and (3.2), the order has been improved to more than four with a 20 percent increase of CPU time. Therefore, for all the non-linear problems, the Padé scheme has been used to compute the partial derivatives of the convection coefficients.

Example 5.8 (Nonlinear Coupled Example)**.**

$$\begin{aligned} &-u_{xx}-u_{yy}+uu_x+vu_y=f(x,y),\\ &-v_{xx}-v_{yy}+uv_x+vv_y=g(x,y), \quad 0<x,y<1, \end{aligned}$$

with exact solution:

$$u(x,y)=e^x+\log(1+y), \quad \text{and} \quad v(x,y)=e^y+\log(1+x).$$

Finally, Algorithm 3.1 developed for the nonlinear model has been applied simultaneously for the coupled equations of (5.8) and the iterative procedure is stopped when the absolute maximum of difference between two consecutive iterative values of u and v are less than 10^{-12}. The obtained solution is compared with the exact solution and the maximum error norms have been presented in the Table 9. A fifth order rate of the scheme confirms the robustness of the scheme in solving the coupled nonlinear equations. The CPU time comparison of the present and [15] shows that once again the developed scheme requires less computational time than the existing schemes.

Table 9: Comparison of mean error, convergence rate and CPU times for Example 5.8.

	Present			Ref. [15]		
No. Nodes	Mean Error	Rate	CPU time	Mean Error	Rate	CPU time
11×11	8.04747(-08)	–	0.1	5.87657(-08)	–	0.15
21×21	2.76758(-09)	4.86	1.69	2.04103(-09)	4.85	2.37
41×41	8.92111(-11)	4.96	24.54	6.71108(-11)	4.93	34.76
81×81	2.13528(-12)	5.38	349.42	2.14944(-12)	4.96	482.07

6 Conclusions

An exponential compact higher order scheme has been developed to solve stationary nonlinear convection-diffusion type differential equations. The scheme is $\mathcal{O}(h^4)$ for one-dimensional and $\mathcal{O}(h^4+k^4)$ for two-dimensional problems. The properties of the developed scheme like accuracy, non-oscillatory behavior and convergence have been tested by solving one and two-dimensional test problems for both variable and nonlinear convection coefficients. These numerical tests demonstrated that the developed scheme has produced fourth order rate and higher order accuracy for both one and two dimensional nonlinear convection-diffusion problems. The spectral analysis carried out on the nonlinear scheme confirms its closeness with SRECHOS of constant convection coefficients [13] demonstrating the robustness of the developed scheme. The CPU time comparisons prove the superiority of the developed scheme over the existing schemes of its class.

Acknowledgments

The author Nachiketa Mishra is greatly indebted to the Council of Scientific and Industrial Research for the financial support 09/084(0389)/2006-EMR-I.

References

[1] A. Shah, H. Guo and L. Yuan, A third-order upwind compact scheme on curvilinear meshes for the incompressible Navier-Stokes equations, Commun. Comput. Phys., 5 (2009), 712–729.
[2] D. N. de G. Allen and R. V. Southwell, Relaxation methods applied to determine the motion, in two dimensions, of a viscous fluid past a fixed cylinder, Quart. J. Mech. Appl. Math., 8 (1955), 129–145.
[3] M. H. Carpenter, D. Gottlieb and S. Abarbanel, Stable and accurate boundary treatments for compact, high-order finite-difference schemes, Appl. Numer. Math., 12 (1993), 55–87.
[4] E. C. Jr. Gartland, Uniform high-order difference schemes for a singularly perturbed two-point boundary value problem, Math. Comput., 48(178) (1987), 551–564.
[5] A. M. Il′in, A difference scheme for a differential equation with a small parameter multiplying the highest derivative (Russian), Math. Zametki., 6 (1969), 237–248.
[6] J. C. Kalita, D. C. Dalal and A. K. Dass, A fully compact HOC simulation of the steady-state natural convection in a square cavity, Phys. Rev. E., 64(6) (2001), 1–13.

[7] S. K. Lele, Compact finite difference schemes with spectral-like resolution, J. Comput. Phys., 103(1) (1992), 16–42.
[8] M. Li, T. Tang and B. Fornberg, A compact fourth-order finite difference scheme for the steady incompressible Navier-Stokes equations, Int. J. Numer. Methods. Fluids., 20 (1995), 1137–1151.
[9] K. Mahesh, A family of high order finite difference schemes with good spectral resolution, J. Comput. Phys., 145 (1998), 332–358.
[10] A. C. R. Pillai, Fourth-order exponential finite difference methods for boundary value problems of convective diffusion type, Int. J. Numer. Methods. Fluids., 37(1) (2001), 87–106.
[11] H.-G. Roos, M. Stynes and L. Tobiska, Numerical Solution of Convection-Diffusion Problems: Convection-Diffusion and Flow Problems, Springer Series in Computational Mathematics 24, Springer-Verlag, New York, 1996.
[12] Y. V. S. S. Sanyasiraju and V. Manjula, Higher order semi compact scheme to solve transient incompressible Navier-Stokes equations, Comput. Mech., 35(6) (2005), 441–448.
[13] Y. V. S. S. Sanyasiraju and N. Mishra, Spectral resolutioned exponential compact higher order scheme (SRECHOS) for convection-diffusion equation, Comput. Methods. Appl. Mech. Eng., 197 (2008), 4737–4744.
[14] W. F. Spotz and G. F. Carey, High-order compact scheme for the steady stream-function vorticity equations, Int. J. Numer. Methods. Eng., 38 (1995), 3497–3512.
[15] Z. F. Tian and S. Q. Dai, High-order compact exponential finite difference methods for convection-diffusion type problems, J. Comput. Phys., 220(2) (2007), 952–974.
[16] D. You, A high-order Padé ADI method for unsteady convection-diffusion equations, J. Comput. Phys., 214(1) (2006), 1–11.